Enhanced Thermal Destruction of Anthracene Vapor upon Laser Irradiation at 248 nm in the 150−800 DegC Range

ARTICLE *in* ENVIRONMENTAL SCIENCE AND TECHNOLOGY · APRIL 1996

Impact Factor: 5.33 · DOI: 10.1021/es950789r · Source: OAI

3 AUTHORS, INCLUDING:

Hubert van den Bergh
École Polytechnique Fédérale de Lausanne
498 PUBLICATIONS **7,577** CITATIONS
SEE PROFILE

Michel J Rossi
Paul Scherrer Institut
260 PUBLICATIONS **6,654** CITATIONS
SEE PROFILE

Environ. Sci. Technol. **1996**, *30,* 1789−1793

Enhanced Thermal Destruction of Anthracene Vapor upon Laser Irradiation at 248 nm in the 150−800 °C Range

ANDREAS THÖNY,
HUBERT VAN DEN BERGH, AND
MICHEL J. ROSSI*

Institute of Environmental Science, Laboratory for Air and Soil Pollution Studies (IGE/LPAS), Swiss Federal Institute of Technology—Lausanne (EPFL), CH-1015 Lausanne, Switzerland

Introduction

One of the primary environmental concerns is proper disposal of toxic as well as municipal waste in view of the large quantities of waste our society is generating. Seventeen of the OECD countries annually generate about 7.7 billion t of municipal and industrial waste, and more than 200 million t of the total waste are classified as toxic or hazardous requiring special disposal techniques (*1*). In addition, there are important quantities of already existing toxic waste awaiting proper disposal.

Searching for highly efficient and cost-effective disposal technology, Graham and Dellinger (*2*) investigated the synergism of combining high temperature processing with UV−VIS radiation in a solar incinerator in the destruction of selected organic compounds that were taken as surrogates for toxic organic waste. They performed laboratory experiments using a strong Xe arc lamp and an air-mass filter to simulate solar radiation and predicted a large increase in the destruction and removal efficiency (DRE) of the combined photon-assisted thermal process as compared to thermal destruction (*3*). Field tests in solar incinerators on 1,2,3,4-TCDD (tetrachlorodibenzo-*p*-dioxin) reported by Glatzmaier et al. (*4*) showed a photon enhancement of up to a factor of 10^4 leading to a fraction remaining f_r of the order of 10^{-6} at 750 °C corresponding to a DRE of 99.9999%, thus satisfying the requirements for the emission of dioxin-like compounds (*5*). Such values can be obtained by traditional incineration technology only when heating to temperatures of the order of 1600 °C or more (*2*).

A more detailed laboratory study on the high-temperature photon-assisted oxidation of monochlorobenzene was published by Graham et al. (*6*). They reported on the photon-assisted DRE using a pulsed dye laser at 280 nm and on a quantitative study of the products of the oxidation process.

We chose anthracene as a test case for photochemical incineration for essentially three reasons: (a) it is a prototypical polycyclic aromatic hydrocarbon; (b) it is a strong absorber at 248 nm, and its temperature dependent absorption spectrum has been measured quantitatively by us (*7*); and (c) it has been found in significant concentrations in flue gas from toxic waste incineration (*8*). We use a KrF rare gas excimer laser at 248 nm as the photon source and an electrically heated tubular oven as the energy input for the flowing gas experiments described below. The determination of the reaction products was not one of the goals of this feasibility study and may be included at a later stage.

* Corrresponding author fax: +41-21-693-36-26; e-mail address: Michel.Rossi@dgr.epfl.ch.

Experimental Section

In our laboratory-scale incineration experiment, we directed a laser beam into a reaction cell placed in a tubular oven (Figure 1). The destruction of anthracene was studied in a flowing gas experiment in which anthracene vapor diluted in 1 atm of filtered compressed air flowed through the all-quartz cell of 50 cm length and 38 mm diameter. The anthracene vapor is generated in a heated sample vessel typically at a temperature of 80 °C containing Raschig rings coated with solid anthracene in order to increase the sample surface to facilitate vaporization. The anthracene vapor density is controlled by the vapor pressure at a given temperature, the rate of evaporation, and the flow rate of compressed air. The air flow rate is set by using a mass flow controller at ambient temperature. The flow determines the gas residence time (t_R) in the cylindrical cell ranging from 1.5 s to several minutes. In order to avoid condensation of anthracene vapor on cold spots in the flow-through reactor, the temperature of the transfer lines and the oven were kept at least 30 °C higher than that of the sample vessel. This requirement determined the lowest attainable temperature of 150 °C for the present experiments.

We collected the fraction of the sample that survives the heated section at the end of the gas flow system. The sample is collected for typically 1 min using a cold trap filled with quartz wool and cooled to a temperature of −78 °C. Subsequently, the content of the trap is dissolved in hexane, and the mass of anthracene in this solution is determined using a common dual-beam UV spectrometer (UVIKON 860) as well as a GC equipped with a FID detector (Varian 3400) as an alternative, albeit more sensitive, detection technique.

The measurement of the destruction enhancement factor (R) defined in eq 1 for a given temperature requires two measurements: the first performed in the absence of laser radiation in order to obtain the fraction of anthracene remaining for the pure thermal process $f_r(0)$, the other in the presence of UV photons obtaining the fraction remaining $f_r(h\nu)$ for the combined photon-assisted thermal process (cf. Figure 2):

$$R = f_r(0)/f_r(h\nu) \qquad (1)$$

The quantities f_r are determined by taking the ratio of the quantity of anthracene flowing into the tubular reactor to the quantity leaving the reactor after either thermal or photon-assisted thermal treatment. The photon-assisted destruction occurred by irradiating along the axis of the cylindrical flow cell with the output of a pulsed KrF excimer laser at 248 nm (Lumonics EX 520) with a typical pulse duration of 12 ns and a pulse energy of 16 mJ measured at the exit window of the reactor. The transmitted average power was adjusted by changing the pulse repetition frequency and was measured using a power meter. As the gas transfer lines are connected to the entrance and the

0013-936X/96/0930-1789$12.00/0

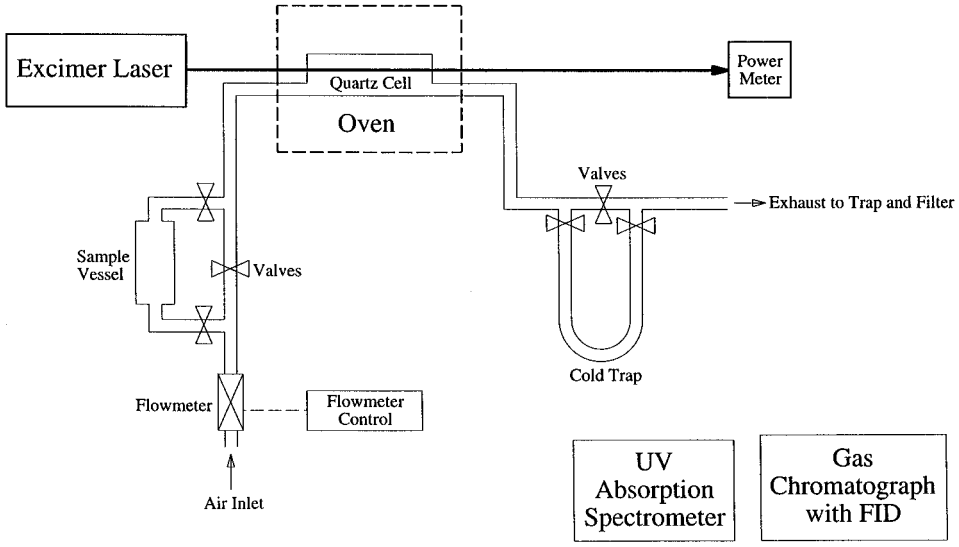

FIGURE 1. Apparatus used for laser-assisted destruction of organic compounds in a flowing gas experiment.

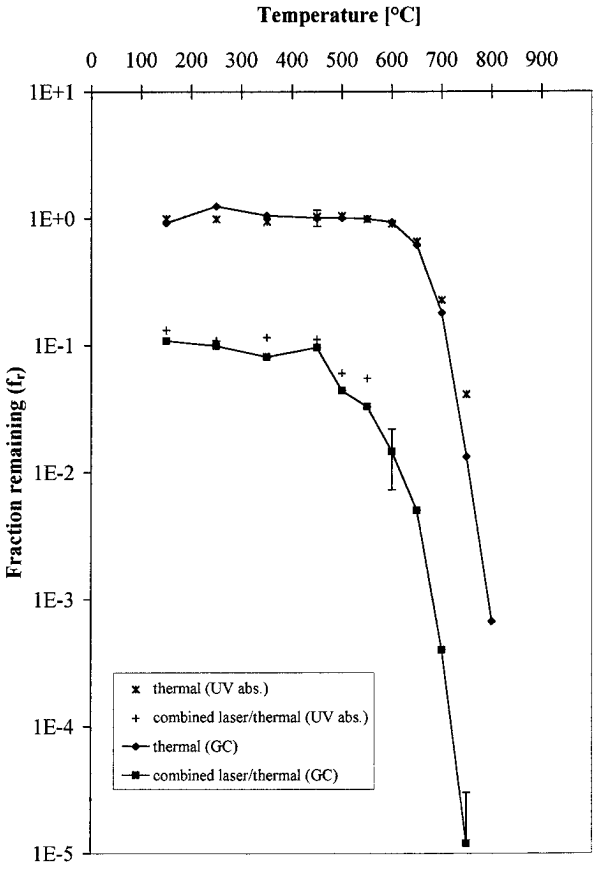

FIGURE 2. Thermal and combined laser-assisted thermal destruction of anthracene for an average laser power of 13 mW/cm^2 analyzed using absorption spectrometry (UV abs.) and GC. Error bars change with temperature and represent typical values.

exit windows of the cylindrical reaction cell, only about two-thirds of the cross section of the cell could be irradiated.

In the case of high extents of anthracene destruction, f_r was determined by GC after prolonged sample collection (up to 1 h) and concentration by solvent evaporation. Subsequently, an aliquot was injected into the GC for analysis. This led to a dynamic measurement range in f_r of 10^5 at this particular anthracene concentration.

Results and Discussion

Figure 2 displays the results of both the thermal as well as the photon-assisted thermal destruction of anthracene in terms of the fraction remaining (f_r) as a function of the temperature of the oven. The average power density at 248 nm and the concentration of anthracene were set to low values of 13 mW/cm^2 and 100 nM at a flow rate of 2 dm^3/min at ambient temperature, respectively. ♦ and ■ represent $f_r(0)$ and $f_r(h\nu)$ corresponding to the pure thermal and the photon-assisted thermal process, respectively. We observe a large relative decrease in $f_r(h\nu)$ in relation to $f_r(0)$ thus resulting in an increase in destruction efficiency R when illuminating with UV photons, typically a factor of 1000 at 750 °C at the applied conditions. Due to the large absorption cross section of anthracene at 248 nm, $f_r(h\nu)$ is already 0.1 at 150 °C whereas $f_r(0)$ starts to decrease only at temperatures in excess of 550 °C.

Using the present experimental method, we attained $f_r(h\nu) = 10^{-5}$ corresponding to 10 ppm relative to an inlet concentration of 6×10^{13} molecules cm^{-3} at ambient temperature. This value for $f_r(h\nu)$ represents our present detection limit for anthracene involving sample concentration through solvent evaporation and prolonged sample collection time. These data extend the range of results for f_r by 2 orders of magnitude compared to data previously published by other authors (*2*, *3*, *6*).

Using our setup, we can only measure the anthracene concentration at the reactor inlet and outlet and the total absorption over the reactor length. The latter is smaller than 10% except for the investigations at high concentrations also displayed in Figure 3. At the higher concentrations, there is an exponential decrease of anthracene as well as of the photon density along the reactor axis. This is expected as the number of anthracene molecules and the number of photons at the reactor entrance are of the same order of magnitude.

The data labeled with an asterisk on a plus in Figure 2 represent experiments where f_r has been determined using UV absorption. It can be seen that both analytical methods yield identical results within experimental error in the concentration ranges where both methods are applicable. The values of f_r determined using UV absorption are found to be slightly larger than the ones measured using GC. This may be due to the potentially non-negligible absorption of

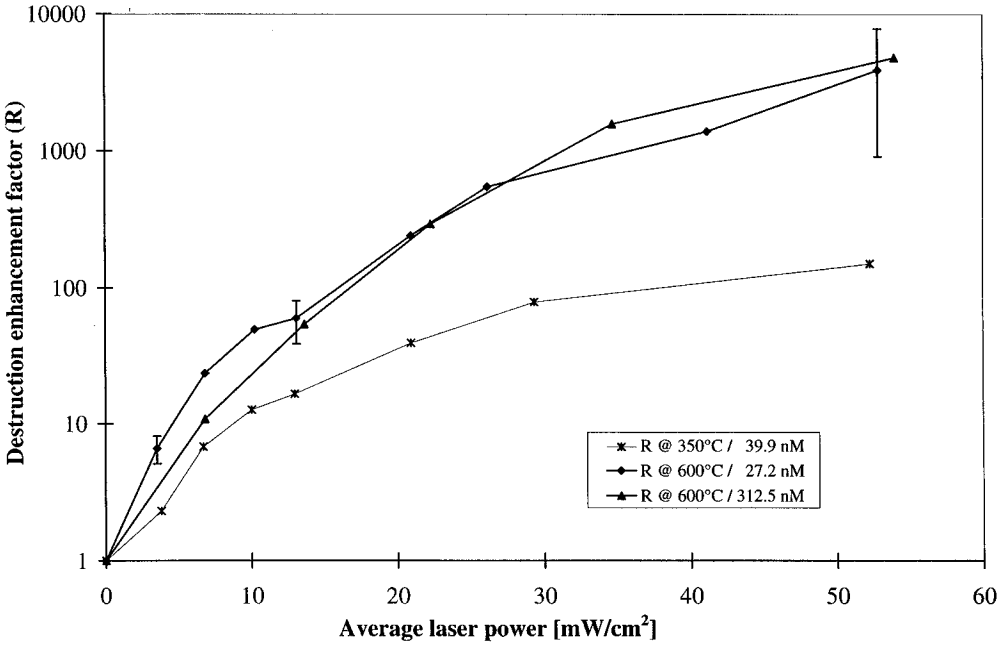

FIGURE 3. Dependence of the destruction enhancement factor on the average laser power for the photon-assisted thermal destruction of anthracene at 350 °C and for two different concentrations at 600 °C. Typical error bars are shown.

TABLE 1

Summary of Spectroscopic and Destruction Data Obtained for Anthracene at Different Temperatures

T (°C)	σ_{248nm} (cm²)	t_R [b] (s)	$f_r(0)$	$f_r(h\nu)$ [c]	R	ϕ
150	6.73E−17	9.84	0.924	0.109	8.5	0.195
250	9.21E−17	7.96	1.248	0.099	12.6	0.208
350	1.29E−16	6.68	1.055	0.081	13.0	0.179
450	1.51E−16	5.76	1.013	0.096	10.6	0.163
500	1.70E−16	5.38	1.011	0.044	23.0	0.207
550	1.76E−16	5.06	0.997	0.033	30.2	0.231
600	1.82E−16[a]	4.77	0.932	0.0146	63.8	0.289
650	2.05E−16[a]	4.51	0.617	0.0048	128.5	0.316
700	2.19E−16[a]	4.28	0.181	0.00038	476.3	0.396
750	2.33E−16[a]	4.07	0.0133	0.000012	1108.3	0.445
800	2.47E−16[a]	3.88	0.00067			

[a] Absorption cross sections calculated by linear regression from values measured for temperatures smaller than 600 °C. E−17 stands for × 10^{-17}. [b] Compressed air flow rate was 2 dm³ min⁻¹ at room temperature. [c] The laser power was kept constant at 13 mW/cm².

the numerous decomposition products contributing to absorption at the wavelength where anthracene is monitored. Therefore, f_r values obtained using UV absorption are only useful for small extents of destruction due to the possible interference of decomposition products in this concentrated solution.

The flow rate of filtered compressed air was held constant in the experiments at all temperatures. As the pressure inside the reaction cell is constant at 1 atm with increasing temperature, the sample concentration as well as the gas phase residence time in the hot reaction cell decrease linearly with increasing temperature: for instance when t_R is set to 9.8 s at 150 °C at a given air flow, it will decrease to 4.8 s at 600 °C (see Table 1). Therefore, plots of f_r as a function of temperature are subject to an additional "hidden" parameter, which is the variation of concentration or residence time. However, this effect cancels out in plots of R vs temperature because both $f_r(h\nu)$ and $f_r(0)$ are affected to the same extent. When data such as displayed in Figure 2 are normalized to the ambient temperature residence time or concentration, the precipitous drop of f_r with increasing temperature would be even more pronounced. From the two series of measurements of $f_r(0)$ and $f_r(h\nu)$ as a function of temperature, we determined an apparent activation energy E_a of 157.4 kJ/mol for the pure thermal and 69.5 kJ/mol for the UV-enhanced thermal destruction at temperatures higher than 650 °C. These values were derived by assuming a first-order rate law for anthracene disappearance. In ancillary experiments it became clear, however, that the rate of disappearance of anthracene follows a complex rate law because the rate constant k derived from the relation

$$[A(t)] = [A]_0 \exp(-kt) \qquad (2)$$

with $f_r(0) = [A(t_R)]/[A]_0$ depended both on the concentration of anthracene as well as on the residence time t_R. Nevertheless, the values for k that were used to compute the activation parameters were obtained at low concentrations and for short residence times in order to keep the extent of secondary chemistry to a minimum. The values for E_a quoted above therefore do not pertain to the elementary unimolecular decomposition of anthracene and merely serve to point out the overall temperature sensitivity for anthracene destruction under our experimental conditions.

The detailed reaction mechanism of photon-assisted incineration is not yet completely understood. The activation energy for unimolecular decomposition out of the first excited singlet state S_1 presumably is significantly smaller than that of the ground electronic state S_0. There are two alternative pathways: decomposition out of the metastable triplet state T_1 or via predissociation from the singlet S_1. However, in view of the short lifetime of S_1 in the nanosecond range or fraction thereof, it is more likely that reaction or thermal decomposition occurs from the lowest triplet state T_1 formed by intersystem crossing from the primary photoproduct. These triplet states may have lifetimes some 3−6 orders of magnitude longer than the S_1 state and are also expected to have a significantly reduced energy barrier for chemical reaction similar to the S_1 state (*3*).

To a first approximation, we may represent the photon-assisted thermal incineration process by a model consisting of a simple competition between the thermal destruction, reaction 3, and the destruction of an electronically excited metastable state of anthracene *A* (here presumed to be the triplet state T_1; reaction 4):

$$A + \text{heat} \rightarrow \text{products} \quad (3)$$

$$A + h\nu \rightarrow \rightarrow {}^3A^*(T_1) + \text{heat} \rightarrow \text{products}' \quad (4)$$

As long as there is no appreciable buildup of product species interacting with anthracene or its excited state, i.e., at small extents of reaction, this mechanism may well represent the rate of destruction of anthracene as a function of temperature and laser power density provided the absorption properties of anthracene as a function of temperature are known.

The reaction mechanism we invoke, reactions 3 and 4, is just a framework for discussion of exploratory results discussed in this paper. Tsang and co-workers have advanced a detailed mechanism for the incineration of polyatomic molecules based on elementary chemical kinetics at high temperatures (*9, 10*). Such a scheme is an ideal tool to assess the efficiency of incineration and the incinerability of polyatomic molecules under any given set of chosen conditions from first principles. The most important practical aspect of such a detailed scheme, however, lies in the predictability of the behavior of complex mixtures under incineration conditions barring any unforeseen kinetic effects such as heterogeneous processes, which may be incorporated into the model at a later time. The ultimate goal of our effort has to be seen in this context as we strive to characterize the kinetic stability of complex organic molecules at moderate temperatures in the presence of UV photons.

In those investigations, where Dellinger and co-workers focused on solar incineration, they were unable to decouple the photon from the thermal energy. We searched therefore for an alternative solution where the photon and the thermal source could be controlled in a more independent fashion in order to provide the basis for a dependable and optimized technology of photon-enhanced incineration similar to the laboratory work by Dellinger and co-workers (*6*).

Figure 3 displays the variation of *R* as a function of laser power at constant temperature for 350 °C and for two conditions at 600 °C. The two curves obtained at 600 °C correspond to different sample concentrations of 27.2 and 312.5 nM at that temperature, respectively, and are indistinguishable within the present experimental uncertainty. At 600 °C, we obtain a destruction enhancement factor *R* of approximately 4000 at an average laser power of 54 mW/cm^2. At 350 °C, *R* is already equal to 150, which points to the efficiency of this photoenhanced destruction reaction.

Using as a model for the disappearance the simple competition between the thermal destruction, reaction 3, and the thermal destruction of the T_1 state of anthracene, reaction 4, we expect a linear relationship between *R* and the laser power in a semilogarithmic representation of the data according to

$$R(T) = \exp[\sigma(T)It\phi(T)] \quad (5)$$

where *I* is the photon flux of the laser radiation at a given wavelength, *t* is the duration of the laser pulse with *It* being the dose per pulse, σ is the absorption cross section, and ϕ is the quantum yield for thermal unimolecular decomposition of anthracene (T_1) at temperature *T*. The assumptions we adopt in this simple model are that the branching ratio between both pathways is linearly dependent on the laser photon flux I and that the overall process is a superposition of two reactions, one of which is independent of *I*.

In order to check the prediction of the simple model presented above (reactions 3 and 4, relation 5) we have determined in a separate experiment the dependence of the absorption cross section σ on the wavelength λ in the UV range of 200−400 nm and for temperatures from 150 up to 550 °C where anthracene starts to decompose. For example we observe an increase in absorption at 248 nm of a factor of 2.6 between 150 and 550 °C due to the red shift of the ^{1}B-band (see Table 1). Generally, it is difficult to predict the trends in absorption with increasing temperature at any one wavelength so that it is most useful in practice if the whole absorption spectrum is recorded. This has been done in the present case by recording the absorption spectrum as a function of temperature using a spectrometer equipped with a CCD camera. Full details of absorption spectra of anthracene at elevated temperatures and other polycyclic aromatic species will be published elsewhere (*7*). Furthermore, we conclude from gas-phase absorption spectroscopy up to temperatures of 700 °C that there is no observable contribution of combustion byproducts.

The results presented in Figure 3 show saturation behavior for *R* vs laser power that is unexpected following the simple mechanistic scheme outlined above. The present experiments seem to indicate a loss of excitation at higher laser powers or a reluctance of a portion of the anthracene molecules to undergo photoenhanced destruction. We checked for the absence of multiphoton effects as well as the absence of concentration quenching at higher laser power densities *I* as the *R* values are independent of sample concentration (cf. Figure 3). The present experiments show that the quantum yield ϕ depends both on the temperature as well as on the applied laser power density: it is increasing with increasing temperature, for instance from 0.20 to 0.45 between 150 and 750 °C, but decreases with increasing laser power, for instance from 0.35 at 3.5 mW/cm^2 to 0.15 at 52.8 mW/cm^2 at 600 °C. As a case in point, quantitative data on anthracene destruction are displayed in Table 1. A closer look at the quantum yields ϕ as a function of temperature reveals a small drop in ϕ between 150 to 450 °C, after which it increases to 0.445. This trend in ϕ is an indication that there may be many contributing processes in addition to reactions 3 and 4 occurring at those temperatures. In addition, we think that the present method of irradiation is subject to an artifact when considering the decrease of ϕ with laser power. From measurements of the photodestruction of other organic compounds performed in our laboratory, we seem to reach a lower limiting value of $f_r = 10^{-6}$ regardless of the applied laser power. This seems to indicate that 1 ppm or so of the organic fraction does not interact with the laser radiation in the present experimental configuration, which presently does not permit homogeneous illumination of the reaction cell.

We are now in a position to extrapolate to destruction conditions at higher temperatures and/or higher laser powers. It seems realistic to expect *R* values of the order

of 10^4-10^6 at 750 °C using an average laser power of 54mW/cm^2 taking the method into the realm of ppb levels of destruction of organic species.

Acknowledgments

The authors like to thank Alfred Neuenschwander and Flavio Comino for their technical and advisory support. This project was supported by the Swiss National Science Foundation under Grant 20-37599.93.

Literature Cited

(1) *OECD Environmental Data, Compendium 1993*. OECD: Paris, Cedex, 1993.
(2) Graham, J. L.; Dellinger B. *Energy* **1987**, *12* (3/4), 303−310.
(3) Graham, J. L.; Dellinger, B. In *Proceedings of the fourth international symposium on Solar thermal technology research development and applications;* Gupta, B. P., Traugott, W. H., Eds.; Hemisphere Publishing Corporation: New York, 1990; pp 391−406.
(4) Glatzmaier, G. C.; Nix, R. G.; Mehos, M. S. *J. Environ. Sci. Health.* **1990**, *A25* (5), 571−581.
(5) Holloway, R. Presented at the 84th Annual Meeting of the Air & Waste Management Association, Vancouver, 1991; Presentation 91-26.12.
(6) Graham, J. L.; Berman, J. M.; Dellinger, B. *J. Photochem. Photobiol. A: Chem.* **1993**, *71*, 65−74.
(7) Thöny, A.; van den Bergh, H.; Rossi, M. J. In *Proceedings of the 89th Annual Meeting of the Air & Waste Management Association*, June 23−28, 1996; Nashville, 1996 (in press).
(8) Wienecke, J.; Kruse, H.; Huckfeldt, U.; Eickhoff, W.; Wassermann, O. *Chemosphere* **1995**, *30* (5), 907−913.
(9) Shaub, W. M.; Tsang, W. *Environ. Sci. Technol.* **1983**, *17* (12), 721−730.
(10) Tsang, W.; Burgess, D., Jr. *Combust. Sci. Technol.* **1992**, *82*, 31−47.

Received for review October 25, 1995. Revised manuscript received February 29, 1996. Accepted March 6, 1996.

ES950789R